ADVANCED MATERIALS
www.advmat.de

Edge Functionalization of Graphene and Two-Dimensional Covalent Organic Polymers for Energy Conversion and Storage

Zhonghua Xiang, Quanbin Dai, Jian-Feng Chen, and Liming Dai**

Edge functionalization by selectively attaching chemical moieties at the edge of graphene sheets with minimal damage of the carbon basal plane can impart solubility, film-forming capability, and electrocatalytic activity, while largely retaining the physicochemical properties of the pristine graphene. The resultant edge-functionalized graphene materials (EFGs) are attractive for various potential applications. Here, a focused, concise review on the synthesis of EFGs is presented, along with their 2D covalent organic polymer (2D COP) analogues, as energy materials. The versatility of edge-functionalization is revealed for producing tailor-made graphene and COP materials for efficient energy conversion and storage.

1. Introduction

It has been predicted that the world will need to double its energy supply by 2050. Nanotechnology has opened up new frontiers in materials science and engineering to meet this challenge by offering a unique enabling technology to create new functionalized materials for energy conversion and storage (e.g., fuel cells, solar cells, batteries, supercapacitors).[1] As a building block for all other multifunctional carbon materials (e.g., 0D buckyballs, 1D nanotubes, 3D graphite), graphene, the one-atom-thick layer of sp^2-bonded, 2D honeycomb lattice of carbon with a fully conjugated structure of alternating C–C and C=C bonds, has attracted tremendous research interest due to its peculiar structure and unique physicochemical properties.[2] Graphene has been demonstrated to exhibit an extremely high carrier mobility (ca. 200 000 $cm^2\ V^{-1}\ s^{-1}$),[3] large specific surface area (2630 $m^2\ g^{-1}$),[4] excellent mechanical strength (breaking strength of 42 N m^{-1} and Yong's modulus of 1.0 TPa),[5] good thermal conductivity (ca. 5000 W $m^{-1}\ K^{-1}$), and superior flexibility.[6] These properties make graphene a promising candidate for a large variety of applications,[7] including energy conversion and storage. Like many other conjugated macromolecules (e.g., 2D conjugated covalent organic polymers (2D CCOPs)), however, pristine graphene without functionalization is insoluble and infusible, which has hindered its practical application. Consequently, various functionalization methods, including basal-plane-functionalization via chemical grafting or noncovalent adsorption, asymmetrical functionalization of the basal plane with different moieties on the opposite graphene surfaces, and edge-functionalization, have been developed for preparing solution-processable graphene sheets.[1] Among them, edge-functionalization is of particular interest as the dangling bonds at the edge of a graphene sheet have been demonstrated to be more reactive than the covalently bonded carbon atoms in the basal plane.[8] Edge-functionalized graphene (EFG) can be soluble, and hence processable, while the physicochemical properties of the pristine graphene can be largely retained. Furthermore, edge-functionalization can also impart the electrocatalytic-activity and/or chemical-reactivity characteristics of the attached chemical moieties for specific applications. However, the research and development of EFGs[9] for device applications is still in its infancy.

On the other hand, 2D covalent organic polymers (COPs)[10] with conjugated macromolecular architectures are analogous to graphene, which can be constructed by controlled synthesis and molecular engineering. Like graphene, 2D CCOPs can also be made soluble by functionalizing with appropriate functional groups at their perimeter (edge),[11] and they are, in essence, edge-functionalized graphene nanoribbon networks with hydrogen atoms/other chemical functionalities as the edge moieties. Here, we present a focused, concise review on recent progress in the development of edge-functionalized graphene and 2D CCOPs for energy conversion (e.g., fuel cells, solar cells) and storage (e.g., batteries).

Prof. Z. Xiang, Prof. L. Dai
BUCT-CWRU International Joint Laboratory
State Key Laboratory of Organic-Inorganic Composites
College of Energy
Beijing University of Chemical Technology
Beijing 100029, China
E-mail: liming.dai@case.edu
Prof. Z. Xiang, Prof. J.-F. Chen
State Key Laboratory of Organic-Inorganic Composites
Beijing University of Chemical Technology
Beijing 100029, China
E-mail: chenjf@mail.buct.edu.cn
Q. Dai, Prof. L. Dai
Center of Advanced Science and Engineering
for Carbon (Case 4Carbon)
Department of Macromolecular Science and Engineering
Case Western Reserve University
10900 Euclid Avenue, Cleveland, OH 44106, USA

DOI: 10.1002/adma.201505788

2. Edge Functionalization of Graphene and 2D CCOPs

Although graphene has been demonstrated as an attractive candidate for energy applications due to its special structure and unique properties, it is rare for graphene-based materials with desirable bulk properties to also possess the necessary surface characteristics specific for certain applications. Therefore, surface functionalization is essential to make graphene materials of good bulk and surface properties as required for efficient energy conversion and storage. Compared to the basal plane with highly delocalized π electrons over the covalently bonded sp^2 hybridized carbon atoms, the edge sites of graphene with dangling bonds have been demonstrated to be more reactive,[8,12] and they can be used for the covalent attachment of various chemical moieties. Unlike functionalization of the graphene basal plane, which often causes significant distortion of the π–π conjugation and the associated physicochemical properties, the graphitic structure and graphene properties can be largely retained by edge modification. Both experimental and theoretical results have revealed certain edge-specific chemistry and properties for graphene nanoribbons.[13] It was found that the edge functionalization of armchair graphene nanoribbon does not significantly affect its bandgap whereas the electronic state of zigzag graphene nanoribbons varies with edge functionalization.[13]

2.1. Edge Functionalization of Graphene by Chemical Exfoliation

Baek and co-workers were the first to report the edge-functionalization of graphite by covalently grafting 4-aminibenzoic acid (ABA) molecules, as organic molecular wedges, directly onto graphite particles in the presence of poly(phosphoric acid) (PPA) in *N*-methyl-2-pyrrolidone, leading to high-yield exfoliation of the 3D graphite into 2D graphene-like sheets.[14] In this particular case, the reaction medium, PPA, could not only protonate the surface of graphite, but also show strong ionic interaction with the ionized graphite surface to delaminate the graphite. Subsequently, carbonium ions ($–C^+=O$) generated on the ABA wedge molecules, in the presence of PPA/P_2O_5, attacked the sp^2 C–H bonds on the edge of the graphite, leading to the formation of EFGs without damaging the crystalline graphene basal plane, which is unreactive to carbonium ions (Scheme (a) in **Table 1**).

2.2. Edge Functionalization of Graphene Oxide

Oxidation–exfoliation of graphite with strong oxidizing reagents (e.g., H_2SO_4, $KMnO_4$), followed by reduction, has been the most widely used procedure for large-scale production of soluble graphene.[15] Solution-processable GO sheets, with reactive carboxylic acid groups at the edge and epoxy/hydroxyl groups on the basal plane, provide a good starting material for the functionalization of graphene, which would otherwise be very difficult, if not impossible, due to its poor solubility. The carboxylic acid groups at the edge of the GO can be used for covalent attachment of various chemical moieties to impart solubility, film-forming capability, and specific properties for device applications, as exemplified by some typical examples listed in Table 1 (Scheme (b)–(d)). This approach can be viewed as potentially promising for large-scale fabrication of soluble graphene sheets with region-specific chemical characteristics.

2.3. Edge Functionalization of Graphene by Ball Milling

Recently, Jeon et al. developed an alternative approach for mass production of edge-carboxylated graphene nanoplatelets (CGnPs) simply by ball milling graphite with dry ice (solid state of carbon dioxide) to produce surface-carboxylated graphite particles.[9a] During the ball milling of graphite, the strong shear forces generated between the high-speed rotating balls caused the mechanochemical cracking of the graphitic C–C bonds, leading to spontaneous incorporation of functional groups on the surface of the broken graphite particles. Owing to the large repulsive forces between the surface carboxylate groups and their strong interaction with polar solvents (e.g., water), the resultant surface-carboxylated graphite particles can be efficiently exfoliated into few-layer edge-carboxylated graphene (ECG) nanosheets in various polar solvents without basal plane damage, as the basal plane is effectively protected by the particle structure during the ball milling prior to the subsequent dissolution exfoliation.[9a]

The edge carboxylate functional groups in the ECG can be readily confirmed by Fourier transform infrared (FTIR) spectroscopy with a strong C=O stretching peak at 1718 cm^{-1}, in conjunction with a unique sharp peak for C–O stretching at 1250 cm^{-1} exclusively arising from O=C–OH.[9a] In contrast, GO exhibits a broad C–O stretching band due to the coexistence of C–OH (hydroxyl), C–O–C (epoxy) and O=C–OH (carboxyl) groups on its basal plane and edge. The obtained ECG also exhibits a large surface area of 389.4 $m^2\ g^{-1}$. ECG film shows an electrical conductivity as high as 1214 S cm^{-1} after thermal decarboxylation.[9a]

Owing to the highly generic nature characteristic of ball-milling technology, various heteroatoms, such as nitrogen and halogen, can be introduced at the edge of graphene nanoplatelets by ball milling of graphite powder in the presence of appropriate chemical(s) other than dry ice in any form (gas, liquid, and/or solid).[16] Indeed, various functional groups, such as halogens (F, Cl, Br, I), amine ($–NH_2$), and sulfonic acid ($–SO_3H$), have been efficiently introduced at the edges of graphene nanoplatelets under similar ball-milling conditions as for ECG. To date, more than 20 edge-functionalized EFGs have been produced by this simple ball-milling approach (Scheme (e) in Table 1).[16,17] Therefore, ball milling can be regarded as a simple, but efficient, approach to a large variety of edge-functionalized graphene nanoplatelets.

2.4. Edge-Functionalized 2D COPs

Graphene can be considered as a 2D conjugated aromatic polymer.[18] Like conventional polymers, therefore, graphene (particularly, graphene nanoribbons) can also be chemically synthesized via various organic synthetic protocols.[19] As shown in **Figure 1**a, a 12 nm graphene nanoribbon was

Adv. Mater. **2016**,
DOI: 10.1002/adma.201505788

Table 1. Representative edge-functionalized graphene for energy applications.

	Scheme for edge functionalization	Applications
(a)	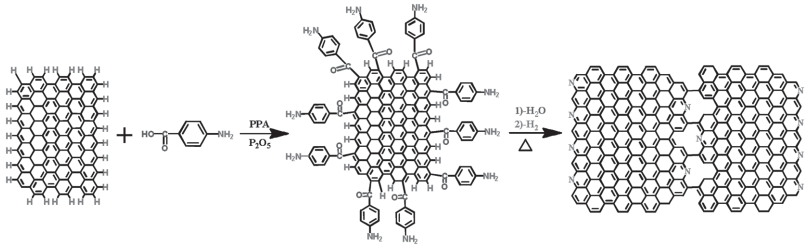	ORR[17c] LIB[47a]
(b)	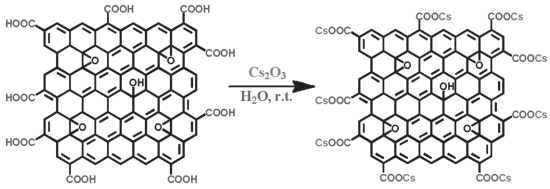	PSC[e)][36a]
(c)	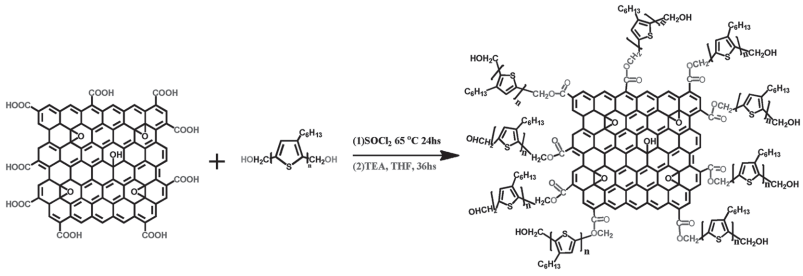	PSC[37]
(d)	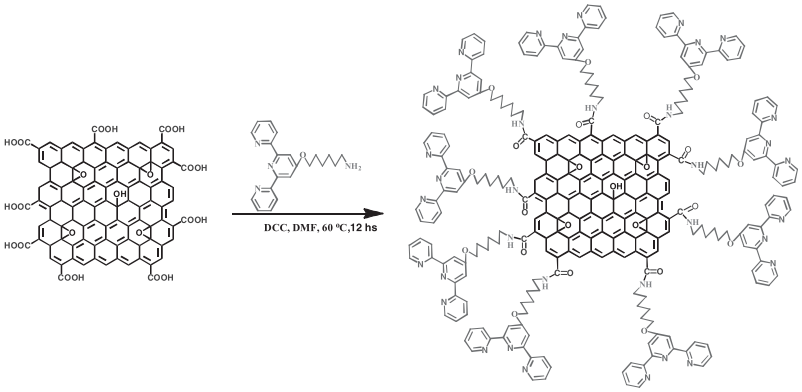	ORR[32b] sb:ORR[51]
(e)	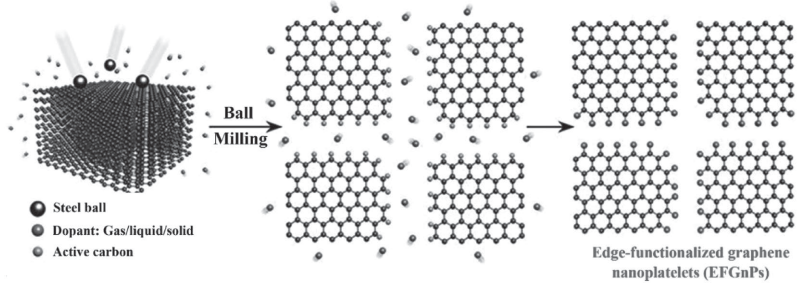	Dopant: Gas: N_2: DSSC[a)] amp; ORR[b)][16a] DSSC[41] H_2: ORR[17a] Cl_2: ORR[16b] LIB[c)][48] DSSC[39] F_2: DSSC amp; LIB[40] NH_3[9a] SO_3: ORR[17a] Liquid: Br_2 ORR[16b] LIB[48] Supercapacitor[52] DSSC[39] Solid: Dry ice(CO_2): ORR,[53] DSSC[41] I_2: ORR[16b] LIB[48] supercapacitor[52] Sulfur: ORR,[34] LSB[d)][49]

[a)]DSSC = dye-sensitive solar cell; [b)]ORR = oxygen reduction reaction; [c)]LIB = Lithium-ion battery; [d)]LSB = lithium–sulfur battery; [e)]PSC = polymer solar cell.

synthesized through the combination of a Suzuki–Miyaura coupling and an intramolecular Scholl reaction, with the incorporation of alkyl chains as edge functional groups to improve the solubility of the resultant graphene nanoribbon.[20] Similarly, hexabenzocoronenes (Figure 1b) have also been chemically synthesized,[21] with more such examples reported in the literature.[19a,22] More generally, 2D CCOPs[10,11,23] can be regarded as edge-functionalized graphene nanoribbon networks

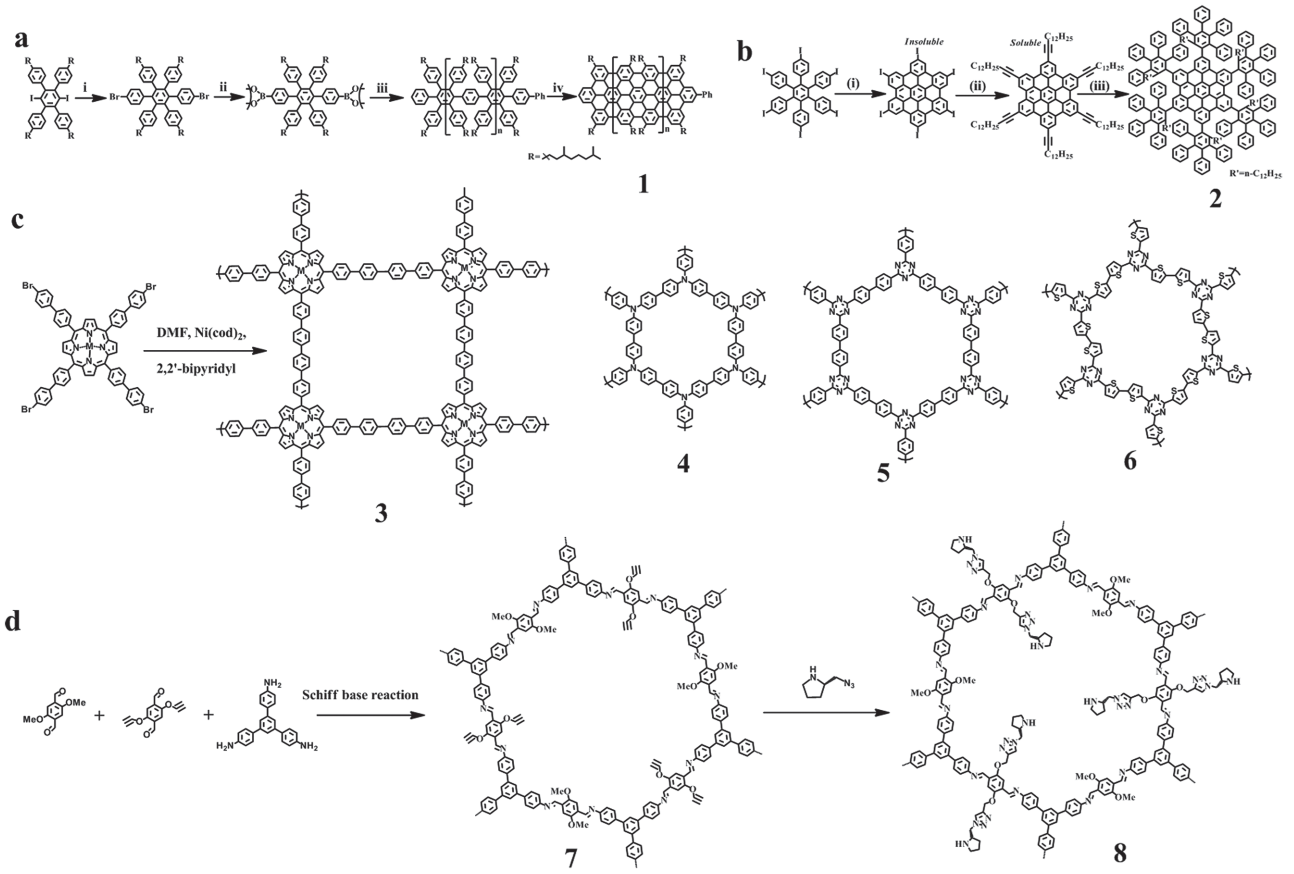

Figure 1. Synthesis of graphene nanoribbons, covalent organic polymers (COPs), and edge-functionalized COPs. a) Reagents and conditions: i) 4-bromophenylboronic acid, $Pd(PPh_3)_4$, aliquat 336, K_2CO_3, toluene, 80 °C, 24 h, 93%.[20] ii) n-BuLi, THF, −78 °C, 1 h; 2-isopropoxy-4,4,5,5-tetramethyl[1,3,2] dioxaborolane, rt, 2 h, 82%. iii) $Pd(PPh_3)_4$, aliquat 336, K_2CO_3, toluene/H_2O, reflux, 72 h to produce compound 1, 75%. iv) $FeCl_3$, CH_2Cl_2/CH_3NO_2, 25 °C, 48 h, 65%. b) Reagents and conditions: i) $FeCl_3$ (24 equiv)/CH_3NO_2, CH_2Cl_2, 24 h, 80–90%; ii) 1-tetradecyne, $Pd(PPh_3)_4$, CuI, piperidine, 50 °C, 82%; iii) tetraphenylcyclopentadienone, diphenyl ether, reflux, 26 h, 72% to produce compound 2.[9c] c) The synthesis of compound 3 (i.e., COP-P-M, M = Fe, Co, and Mn[23a]) via Ni(0) catalyzed Yamamoto-type Ullmann cross-coupling reaction. Compounds 4, 5, 6 refer to COP-2,[23e] 4,[23e] T,[23b] respectively. d) Synthesis of compound 8, i.e., chiral COFs ([(*S*)-P_y]$_x$-TPB-DMTP-COFs, x = 0.17, 0.34, and 0.50;[24] 2,5-dimethoxyterephthalaldehyde (DMTA); 1,3,5-tri-(4-aminophenyl) benzene (TAPB); 2,5-bis(2-propynyloxy) terephthalaldehyde (BPTA); (*S*)-Py sites) via channel-wall engineering using a three-component condensation followed by a click reaction.

with hydrogen atoms/other chemical functionalities as the edge moieties. As shown in Figure 1c,d, conjugated precursor molecules can be covalently bonded (e.g., via B–O and/or C–N), with or without different organic linkers, into various fully or partially conjugated 2D COPs with controllable porosity and pore size.[11] Functional groups from the organic linkers (Figure 1d)[24] can be used for further chemical functionalization to prepare edge-functionalized COPs with different edge moieties.[25] 2D COPs with a tailor-made chemical structure and ultrahigh specific surface area are useful for gas (e.g., H_2) storage[26] and even electrocatalysis in energy devices (e.g., fuel cells).[24,27] Because of their fully conjugated and highly ordered network structures, 2D CCOPs can readily form 2D crystal sheets, which can be exfoliated into few-layer or even single-layer sheets,[10a,28] attractive for electronic and many other applications.[10,29] Of particular interest, 2D CCOPs hold great promise as a class of new energy materials due to their controllable conjugated 2D architectures, high porosity, and multi-edge functionalities. Below, we present a focused review to illustrate the potentials of EFGs and 2D CCOPs for energy-related applications.

3. EFGs and 2D CCOPs for Energy Conversion and Storage

3.1. Fuel Cells

Fuel cells are clean energy devices that can convert chemical energy directly into electricity at a high efficiency and produce water as the only by-product by reducing oxygen gas at the cathode and oxidizing fuel (e.g., H_2 gas) at the anode.[1] The oxygen reduction reaction (ORR) plays a key role in controlling the fuel-cell performance.[1,4,30] Although platinum (Pt)-based catalysts have long been regarded as the best catalyst for the ORR, the prohibitive cost and scarcity of the precious-metal catalysts needed for catalyzing the ORR in fuel cells have largely hindered the development of fuel-cell clean-energy technology. In this context, the discovery of carbon nanomaterials as low-cost, metal-free ORR catalysts with extraordinary performance is important.[1,30,31] As we shall see later, the ball-milling method has allowed large-scale production of edge-functionalized (or edge-doped) graphene sheets at low cost, as efficient metal-free

Adv. Mater. **2016**,
DOI: 10.1002/adma.201505788

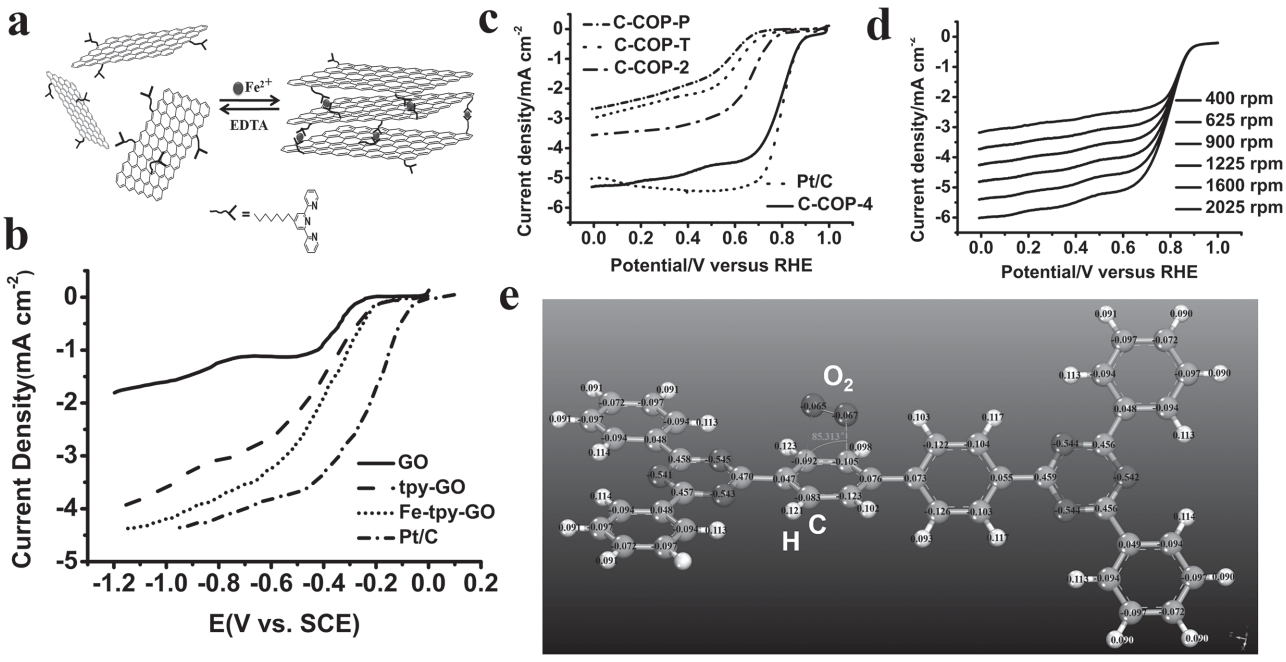

Figure 2. a) Schematic illustration of the complexation–decomplexation (self-assembling) process of tpy-GO. b) Linear sweep voltammetry (LSV) curves for oxygen reduction at the GO, tpy-GO, Fe-tpy-GO, and Pt/C electrodes in an O_2-saturated 0.1 M KOH solution at a scan rate of 10 mV s^{-1}. The electrode rotation speed is 1600 rpm. The current–time (*i–t*) chronoamperometric responses for the ORR at the Fe-tpy-GO and Pt/C electrodes in an O_2-saturated 0.1 M KOH solution at –0.3 V versus SCE. Reproduced with permission.[32b] Copyright 2014, Wiley-VCH. c) LSV curves of COP graphene in O_2-saturated 0.1 M KOH at 1600 rpm at a sweep rate of 5 mV s^{-1}. d) LSV curves of C-COP-4 in O_2-saturated 0.1 M KOH with different speeds at a scan rate of 5 mV s^{-1}. e) Calculated charge distributions for the cluster for optimal O_2 adsorbed in COP-4 graphene. The measured distance is presented in Angstroms, and the measured angle is presented in degrees. Reproduced with permission.[23b] Copyright 2014, Wiley-VCH.

ORR catalysts with an excellent long-term durability and tolerance to methanol crossover/CO poisoning effects.[30c,31]

Generally speaking, doping carbon nanomaterials with heteroatoms (e.g., nitrogen) can cause electron modulation to provide desirable electronic structures for catalytic and many other potential applications.[4,30] Since the discovery by Dai and co-workers in 2009 that nitrogen-doped vertically aligned carbon nanotubes (VA-NCNTs) can efficiently catalyze a four-electron ORR process,[31] many new metal-free ORR catalytic materials of active centers associated with doping-induced positively charged carbon atoms have been developed for fuel cells and many other applications, including metal–air batteries and solar cells.[4,30] With a similar atomic structure and size to, but different electron negativity from, that of carbon, nitrogen was considered as one of the most effective dopants to enhance the ORR activity of graphitic carbon materials.[30–32] The ball-milling approach has been used to prepare not only N-doped EFGs[16a] but also EFGs edge-doped with many other heteroatoms for the ORR, including EFGs edge-functionalized/doped with hydrogen (HGnP), sulfonic acid groups (SGnP), and carboxylic acid/sulfonic acid groups (CSGnP).[17,30c] These EFGs exhibit ORR electrocatalytic activity in the order of SGnP > CSGnP > CGnP > HGnP > pristine graphite, which suggests that both the oxygen diffusion kinetics and the edge polarity of the heteroatom-doped EFGs can significantly contribute to the ORR. In addition to the doping-induced charge-density redistribution,[30] the spin effect is another important issue contributing to the ORR activity.[33] In the case of edge-halogenated graphene nanoplatelets (XGnP; X = Br, Cl, and I),[16b] the experimentally measured electrocatalytic activities for the ORR are in the order of IGnP > BrGnP > ClGnP. First-principles calculations indicate that the efficiency of the charge transfer between the edge-doped halogen and the adsorbed O_2 follows the atomic size in the order of Cl < Br < I, and that the electronic spin density is most prominent for the case of IGnP, leading to the best catalytic activity for IGnP. Because of the almost identical electronegativity of sulfur (χ_S = 2.58) and carbon (χ_C = 2.55), S-doping of EFGs should not induce any charge transfer, and hence no ORR activity. However, ORR activities have also been observed for S-doped EFGs due to the doping-induced spin redistribution.[34]

Along with EFGs prepared by ball milling, chemically synthesized EFGs and 2D CCOPs have also been demonstrated to show good ORR activities. In this regard, Baek and co-workers prepared a 4-aminobenzoyl EFG by a "direct" Friedel–Crafts acylation reaction in a poly(phosphoric acid)/phosphorus pentoxide medium with "pristine" graphite and subsequent pyrolyzation at 900 °C in an inert atmosphere.[17c] Furthermore, Song et al. prepared 3D graphene architectures from terpyridine-functionalized EFG via covalently grafting terpyridine groups at the edge of GO, followed by complexation with various metal ions (e.g., Fe, and Ru).[32b] The resultant 3D graphene showed significantly improved electroactivity for the ORR with respect to pristine GO (**Figure 2**a,b) and an electron-transfer number of 3.63–3.92 for Fe-tpy-GO at potential ranging from –0.7 to –0.5 V (vs saturated calomel electrode (SCE)). Using various N-containing molecular precursors (e.g., triazine derivatives) as building blocks, Xiang and co-workers also synthesized a class

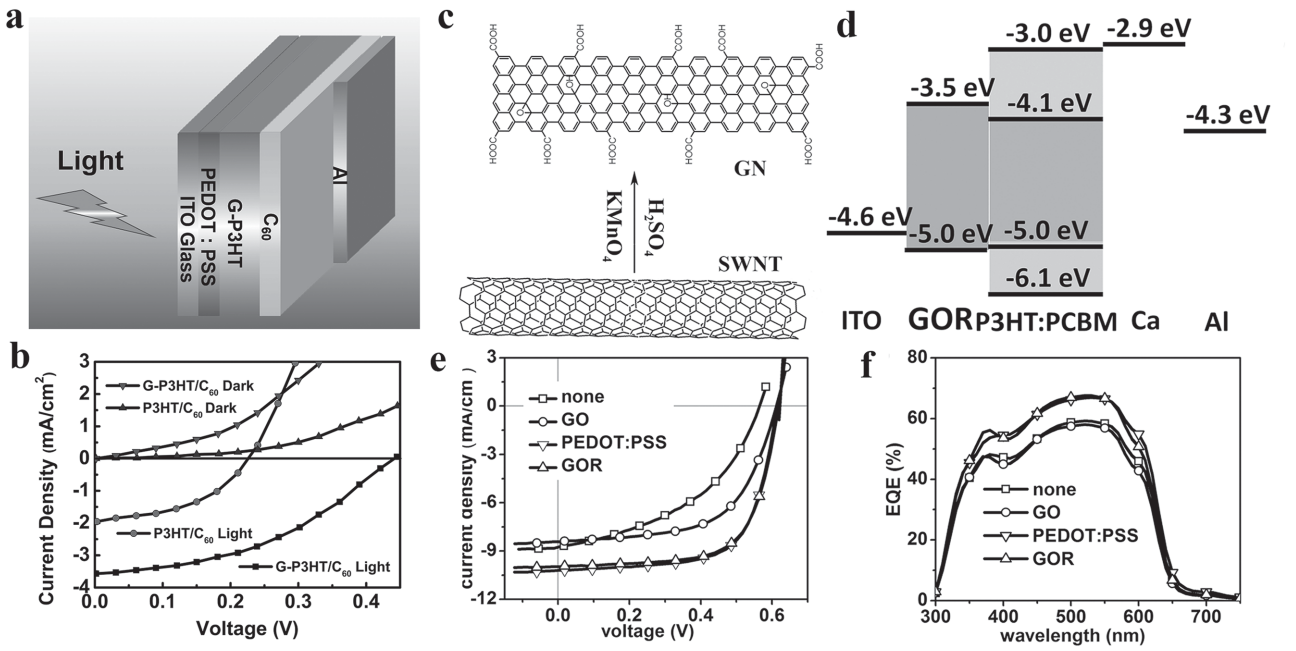

Figure 3. a) Schematic diagram of a ITO/PEDOT:PSS/G-P3HT/C_{60}/Al photovoltaic device. b) Current–voltage characteristics of the photovoltaic devices using P3HT/C_{60} or G-P3HT/C_{60} as the active layer. Reproduced with permission.[37] Copyright 2010, American Chemical Society. c) Schematic illustration of synthesizing GN from oxidative unzipping of SWCNTs. d) Device energy-level alignment for the graphene-nanoribbon-based PSC device of the ITO/GN/P3HT:PCBM (200 nm)/Ca (20 nm)/Al (100 nm) structure. e) The current-density–voltage (*J*–*V*) curves. f) The EQE curves under AM1.5G illumination. Reproduced with permission.[38] Copyright 2014, Wiley-VCH.

of new 2D CCOP networks with precisely controlled locations of N atoms and hole size.[23a,b] Subsequent carbonization of the 2D CCOP networks led to the formation of well-controlled N-doped holey graphene nanosheets. The combined experimental and theoretical approach showed that the N-doped holey graphene nanosheets from 2D CCOPs are promising for efficient energy conversion and storage, particularly as efficient metal-free catalysts for the ORR in fuel cells (Figure 2c–e). This work represents a new strategy to location control of N-dopant heteroatoms in the N-doped graphene structure, which, otherwise, is impossible to achieve with conventional N-doping techniques. Moreover, certain single- and/or multi-nonprecious-metal-embedded (e.g., Co, Fe) COP materials have also been demonstrated to show high electrocatalytic activities for the ORR.[23a,35] The ORR mechanism in these system deserves further investigation.

3.2. Solar Cells

Polymer solar cells (PSCs) offer a low-cost, large-area, and lightweight alternative energy source by spin-coating, ink-jet printing, or roll-to-roll printing the photovoltaic active materials even on flexible plastic electrodes. Although significant progress has been made during the past several decades, the power conversion efficiencies (PCEs) for state-of-the-art PSCs still need to be further improved for commercial applications. As is well known, the photovoltaic effect in a PSC involves the generation of electrons and holes under illumination, and subsequent charge transport and collection at opposite electrodes.[36] To improve the device efficiency of PSCs, therefore, one needs to enhance the charge transport and charge-collection efficiencies. Because of the large specific surface area and high charge mobility for both electrons and holes, graphene and its derivatives (especially EFGs) have been used as a new class of charge-transport and extraction materials in PSCs.[36a] Of particular interest, Yu et al. have covalently grafted regioregular poly(3-hexylthiophene) (P3HT) chains onto carboxylic groups at the GO edge via an esterification reaction (Scheme (c) in Table 1).[37] A bilayer PSC based on the solution-cast P3HT-grafted GO sheets (G-P3HT)/C_{60} heterostructure showed a 2-fold enhancement of PCE with respect to the P3HT/C_{60} counterpart due to the EFG-induced enhancement in charge transport (**Figure 3**a,b).[37] Furthermore, GO and its derivatives have also been studied as hole-/electron-extraction materials in PSCs.[36b] Knowing that GOs can serve as an excellent hole-extraction material with a work function of –4.7. eV, Liu et al., neutralized –COOH groups at the GO edge with cesium (Cs, Scheme (b) in Table 1). They found that the resultant cesium-neutralized graphene oxide is an excellent electron-extraction layer, attributable to the work-function change from –4.7 eV for GO to –4.0 eV for GO-Cs.[36] Similarly, graphene nanoribbons with appropriate edge groups have also been demonstrated to be efficient hole-extraction materials for PSCs (Figure 3c).[38] The same highest occupied molecular orbital (HOMO) (–5.0 eV) level of the edge-carboxylated graphene nanoribbon as that of the donor material, poly(3-hexylthiophene) (–5.0 eV), and the relatively higher lowest unoccupied molecular orbital (LUMO) (–3.5 eV) level of the edge-carboxylated graphene nanoribbon than that of the acceptor material, phenyl-C61-butyric acid methyl ester (PCBM) (–4.1 eV) can effectively improve hole extraction and electron blocking (Figure 3d), and hence a minimized possible

Adv. Mater. **2016**,
DOI: 10.1002/adma.201505788

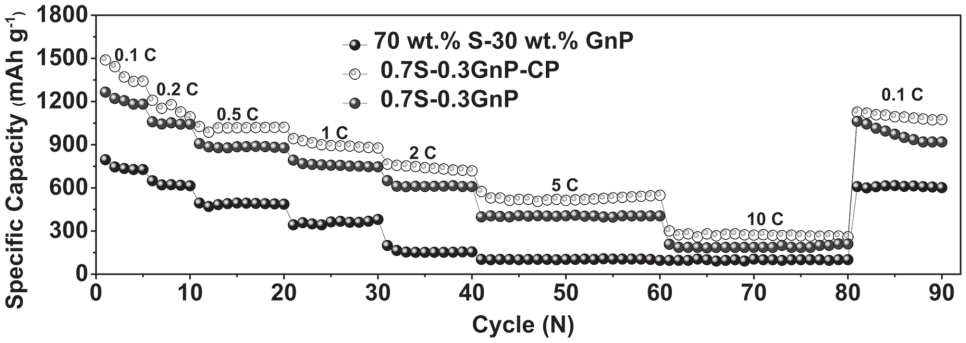

Figure 4. Rate capabilities of LSB based on S-GnPs cathode at 2 C (3350 mA h g^{-1}) in the voltage range of 1.5–3.0 V. Reproduced with permission.[49] Copyright 2014, American Chemical Society.

charge combination loss at the anode and a high overall cell performance (Figure 3e,f).

Due to their high electrical conductivity and electrocatalytic activity, certain EFGs have also been used as highly efficient counter electrodes to replace Pt in dye-sensitive solar cells (DSSCs) with performances comparable to or even better than that of conventional Pt-based DSSCs. For instance, a DSSC based on a nitrogen-edge-doped graphene nanoplatelet (NGnP) cathode showed a PEC of 9.34% (PEC = 8.85% for the Pt-based counterpart).[16a] DSSCs with an IGnP counter electrode or an FGnP counter electrode exhibited fill factors (FFs) of 71.3%[39] and 71.5%,[40] and PCEs of 10.31%[39] and 10.01%,[40] respectively. Edge-carboxylated graphene nanoplatelets (ECGnPs)- or NGnP-based DSSCs also showed high performance (FF = 74.4%, PCE = 9.31% for ECGnPs;[41] and FF = 71.9%, PCE = 10.27% for NGnP[42]).

Along with the development of linear donor–acceptor (D–A) type conjugated polymers of a low bandgap for PSC applications,[36b] the development of high-performance PSCs based on 2D CCOP analogous with donor polymers as the backbone and acceptor units pendant as the side chains/branches has attracted a great deal of interest in the solar-cell community.[43] Recently, highly efficient PSCs have also been developed from a single-layer porphyrin-based 2D microporous, crystalline and indirect bandgap metal–organic framework (MOF) film with a high photovoltaic efficiency and charge mobility due to extended π-electron delocalization.[44] Particularly, the well-defined periodic ordering of conjugated chains in semiconducting 2D CCOPs combine chemical stability and high hole mobility, leading to promising applications in solar cells.[10c,45] As far as the published work is concerned, it would be unfair to comment that not much has been achieved in this area. There remains, however, much work to do.

3.3. Lithium Batteries

Energy-storage devices, especially lithium-ion batteries (LIBs),[1,46] are just as important as energy-conversion devices, such as fuel cells and solar cells discussed above. To improve the charge/discharge rate of LIBs, and hence the device performance, it is important to enhance the kinetics of lithiation and/or delithiation of electrode materials. In this regard, EFGs have been exploited as efficient electrode materials in high-performance batteries due to their high conductivity in the basal plane and abundant active sites at the edge. By selectively controlling the peripheral *d*-spacing through edge-functionalization of graphite in the presence of P_2O_5 and poly(phosphoric acid),[47] Baek and co-workers demonstrated an almost two-fold increase in the capacity or energy density of a LIB from 110 to 190 mA h g^{-1} at a 50 C discharge rate. Subsequently, Xu et al. prepared edge-selectively halogenated graphene nanoplatelets (XGnPs) by ball milling as efficient anode materials to increase the energy density of LIBs.[48] These authors found that the introduction of halogen atoms could not only contribute to the good reversible capacity or cyclability, but also facilitate lithium extraction/insertion.[48] In particular, the IGnP electrode was found to deliver an initial charge capacity of 562.8 mA h g^{-1} at 0.5 C in the voltage range of 0.02–3.0 V, with a high retention rate of 84% even after 500 cycles.

Compared with LIBs, lithium–sulfur batteries (LSBs) exhibit a higher theoretical capacity (ca. 1675 mA h g^{-1}) and energy density (ca. 2600 W h kg^{-1}). However, sulfur-based cathode materials are still suffering from multiple drawbacks, including their low electrical conductivity, large volume expansion, and easy dissolution of sulfur into the electrolyte solution and/or deposition on the lithium anode surface to increase the resistance and shorten the cycle life.[49] To overcome these drawbacks, Xu et al. used sulfur-edge-doped graphene nanoplatelets (S-GnPs) produced by ball milling 70% sulfur with 30 wt% graphite as efficient cathode materials for LSBs.[49] LSB cells based on the S-GnP cathode were found to deliver a high initial reversible capacity of 1265.3 mA h g^{-1} at 0.1 C in the voltage range of 1.5–3.0 V with an excellent rate capability, and a high reversible capacity of 966.1 mA h g^{-1} at 2 C, with a low capacity decay rate of 0.099% per cycle over 500 cycles (**Figure 4**), which outperformed current state-of-the-art cathode materials for LSBs. These results clearly indicate that edge-doped S-GnPs have great potential for next-generation high-performance LSBs. Meanwhile, the tunable pore size in COP materials allows for the incorporation of S into their nanopores to reduce/eliminate soluble polysulfides shuttling between the anode and the cathode and to improve the cycling performance of LSBs.[50] Although recent studies show promise for the use of edge-functionalized graphene and 2D COPs as efficient cathode materials in LSBs, it is too early to celebrate, as the ultimate goal is still not in sight.

4. Concluding Remarks

As discussed above, edge-functionalized graphene and 2D covalent organic polymers with conjugated networks of tunable edge-functional groups possess unique optoelectronic and electrocatalytic properties useful for efficient energy conversion and storage. Edge-functionalization with minimal carbon basal plane damage can further broaden their potential applications by introducing various specific chemical moieties at the edge of a graphene sheet and along the network of 2D covalent organic polymers to impart solubility, film-forming capability, electrocatalytic activity, and/or chemical reactivity. Here, we have revealed the versatility of edge-functionalization for producing tailor-made graphene and covalent organic polymers for efficient energy conversion and storage. Compared with edge-functionalized graphene, however, the development of covalent organic polymers as energy materials is still in its infancy. The synthesis of soluble 2D CCOPs with tunable bandgaps remains challenging. If realized, however, the availability of processable tailor-made 2D CCOPs could significantly facilitate their applications in energy-related and many other devices. Continued research in this exciting field should be very fruitful.

Acknowledgements

The authors would like to thank colleagues and collaborators for their work cited in this article. This work was supported by National Hi-tech R&D Program of China (No. 863 Program, 2012AA101809); NSF of China (51502012); Beijing Natural Science Foundation (2162032); The Start-Up Fund for Talent Introduction of Beijing University of Chemical Technology (No. buctrc201420); Talent cultivation of the State Key Laboratory of Organic-Inorganic Composites; the Fundamental Research Funds for the Central Universities (ZY1508);The 111 Project (B14004); NSF, AFOSR-DoD-MURI, and DAGSI.

Received: November 23, 2015
Revised: December 17, 2015
Published online:

[1] L. Dai, *Acc. Chem. Res.* **2013**, *46*, 31.
[2] a) A. K. Geim, K. S. Novoselov, *Nat. Mater.* **2007**, *6*, 183; b) A. K. Geim, *Angew. Chem. Int. Ed.* **2011**, *50*, 6966.
[3] a) K. S. Novoselov, A. K. Geim, S. V. Morozov, D. Jiang, Y. Zhang, S. V. Dubonos, I. V. Grigorieva, A. A. Firsov, *Science* **2004**, *306*, 666; b) X. Du, I. Skachko, A. Barker, E. Y. Andrei, *Nat. Nanotechnol.* **2008**, *3*, 491.
[4] L. Dai, D. W. Chang, J.-B. Baek, W. Lu, *Small* **2012**, *8*, 1130.
[5] C. Lee, X. D. Wei, J. W. Kysar, J. Hone, *Science* **2008**, *321*, 385.
[6] D. A. Dikin, S. Stankovich, E. J. Zimney, R. D. Piner, G. H. B. Dommett, G. Evmenenko, S. T. Nguyen, R. S. Ruoff, *Nature* **2007**, *448*, 457.
[7] a) K. S. Novoselov, A. K. Geim, S. V. Morozov, D. Jiang, M. I. Katsnelson, I. V. Grigoriev, S. V. Dubonos, A. A. Firsov, *Nature* **2005**, *438*, 197; b) R. M. Westervelt, *Science* **2008**, *320*, 324.
[8] A. Shen, Y. Zou, Q. Wang, R. A. W. Dryfe, X. Huang, S. Dou, L. Dai, S. Wang, *Angew. Chem. Int. Ed.* **2014**, *53*, 10804.
[9] a) I. Y. Jeon, Y. R. Shin, G. J. Sohn, H. J. Choi, S. Y. Bae, J. Mahmood, S. M. Jung, J. M. Seo, M. J. Kim, D. W. Chang, L. M. Dai, J. B. Baek, *Proc. Natl. Acad. Sci. USA* **2012**, *109*, 5588; b) X. Y. Yang, X. Dou, A. Rouhanipour, L. J. Zhi, H. J. Rader, K. Mullen, *J. Am. Chem. Soc.* **2008**, *130*, 4216; c) J. S. Wu, A. Fechtenkotter, J. Gauss, M. D. Watson, M. Kastler, C. Fechtenkotter, M. Wagner, K. Mullen, *J. Am. Chem. Soc.* **2004**, *126*, 11311.
[10] a) Z. H. Xiang, D. P. Cao, L. M. Dai, *Polym. Chem.* **2015**, *6*, 1896; b) Z. H. Xiang, D. P. Cao, *J. Mater. Chem. A.* **2013**, *1*, 2691; c) G. Wan, Fu. Yu'ang, J. N. Guo, Z. H. Xiang, *Acta Chim. Sinica* **2015**, *73*, 557.
[11] Z. H. Xiang, R. Mercado, J. M. Huck, H. Wang, Z. H. Guo, W. C. Wang, D. P. Cao, M. Haranczyk, B. Smit, *J. Am. Chem. Soc.* **2015**, *137*, 13301.
[12] a) W. J. Yuan, Y. Zhou, Y. R. Li, C. Li, H. L. Peng, J. Zhang, Z. F. Liu, L. M. Dai, G. Q. Shi, *Sci. Rep.* **2013**, *3*, 2248; b) W. Lu, J. B. Baek, L. Dai, *Carbon Nanomaterials for Advanced Energy Systems*, Wiley, Hoboken, NJ, USA **2015**.
[13] a) J. H. Warner, Z. Liu, K. He, A. W. Robertson, K. Suenaga, *Nano Lett.* **2013**, *13*, 4820; b) T. Enoki, S. Fujii, K. Takai, *Carbon* **2012**, *50*, 3141; c) A. Orlof, J. Ruseckas, I. V. Zozoulenko, *Phys. Rev. B* **2013**, *88*, 125409; d) C. O. Girit, J. C. Meyer, R. Erni, M. D. Rossell, C. Kisielowski, L. Yang, C.-H. Park, M. F. Crommie, M. L. Cohen, S. G. Louie, A. Zettl, *Science* **2009**, *323*, 1705; e) X. Jia, M. Hofmann, V. Meunier, B. G. Sumpter, J. Campos-Delgado, J. M. Romo-Herrera, H. Son, Y.-P. Hsieh, A. Reina, J. Kong, M. Terrones, M. S. Dresselhaus, *Science* **2009**, *323*, 1701.
[14] E. K. Choi, I. Y. Jeon, S. Y. Bae, H. J. Lee, H. S. Shin, L. M. Dai, J. B. Baek, *Chem. Commun.* **2010**, *46*, 6320.
[15] a) K. R. Paton, E. Varrla, C. Backes, R. J. Smith, U. Khan, A. O'Neill, C. Boland, M. Lotya, O. M. Istrate, P. King, T. Higgins, S. Barwich, P. May, P. Puczkarski, I. Ahmed, M. Moebius, H. Pettersson, E. Long, J. Coelho, S. E. O'Brien, E. K. McGuire, B. M. Sanchez, G. S. Duesberg, N. McEvoy, T. J. Pennycook, C. Downing, A. Crossley, V. Nicolosi, J. N. Coleman, *Nat. Mater.* **2014**, *13*, 624; b) Y. Sun, Q. Wu, G. Shi, *Energ Environ. Sci.* **2011**, *4*, 1113.
[16] a) I. Y. Jeon, H. J. Choi, M. J. Ju, I. T. Choi, K. Lim, J. Ko, H. K. Kim, J. C. Kim, J. J. Lee, D. Shin, S. M. Jung, J. M. Seo, M. J. Kim, N. Park, L. Dai, J. B. Baek, *Sci. Rep.* **2013**, *3*, 2260; b) I. Y. Jeon, H. J. Choi, M. Choi, J. M. Seo, S. M. Jung, M. J. Kim, S. Zhang, L. Zhang, Z. Xia, L. Dai, N. Park, J. B. Baek, *Sci. Rep.* **2013**, *3*, 1810.
[17] a) I. Y. Jeon, H. J. Choi, S. M. Jung, J. M. Seo, M. J. Kim, L. M. Dai, J. B. Baek, *J. Am. Chem. Soc.* **2013**, *135*, 1386; b) I.-Y. Jeon, S.-Y. Bae, J.-M. Seo, J.-B. Baek, *Adv. Funct. Mater.* **2015**, *25*, 6961; c) I. Y. Jeon, D. S. Yu, S. Y. Bae, H. J. Choi, D. W. Chang, L. M. Dai, J. B. Baek, *Chem. Mater.* **2011**, *23*, 3987.
[18] T. Chen, L. M. Dai, *Mater. Today* **2013**, *16*, 272.
[19] a) J. Wu, W. Pisula, K. Muellen, *Chem. Rev.* **2007**, *107*, 718; b) J. Cai, P. Ruffieux, R. Jaafar, M. Bieri, T. Braun, S. Blankenburg, M. Muoth, A. P. Seitsonen, M. Saleh, X. Feng, K. Muellen, R. Fasel, *Nature* **2010**, *466*, 470.
[20] X. Yang, X. Dou, A. Rouhanipour, L. Zhi, H. J. Raeder, K. Muellen, *J. Am. Chem. Soc.* **2008**, *130*, 4216.
[21] J. Wu, L. M. Xie, Y. G. Li, H. L. Wang, Y. J. Ouyang, J. Guo, H. J. Dai, *J. Am. Chem. Soc.* **2011**, *133*, 19668.
[22] a) Q. Tang, Z. Zhou, Z. Chen, *Nanoscale* **2013**, *5*, 4541; b) H. Jiang, *Small* **2011**, *7*, 2413.
[23] a) Z. H. Xiang, Y. H. Xue, D. P. Cao, L. Huang, J. F. Chen, L. M. Dai, *Angew. Chem. Int. Ed.* **2014**, *53*, 2433; b) Z. H. Xiang, D. P. Cao, L. Huang, J. L. Shui, M. Wang, L. M. Dai, *Adv. Mater.* **2014**, *26*, 3315; c) Z. H. Xiang, X. Zhou, C. H. Zhou, S. Zhong, X. He, C. P. Qin, D. P. Cao, *J. Mater. Chem.* **2012**, *22*, 22663; d) Z. H. Xiang, D. P. Cao, W. C. Wang, W. T. Yang, B. Y. Han, J. M. Lu, *J. Phys. Chem. C.* **2012**, *116*, 5974; e) Z. H. Xiang, D. P. Cao, *Macromol. Rapid Commun.* **2012**, *33*, 1184; f) J. W. Colson, W. R. Dichtel, *Nat. Chem.* **2013**, *5*, 453.
[24] H. Xu, J. Gao, D. Jiang, *Nat. Chem.* **2015**, *11*, 905.
[25] a) S. M. Cohen, *Chem. Rev.* **2012**, *112*, 970; b) H. Xu, X. Chen, J. Gao, J. Lin, M. Addicoat, S. Irle, D. Jiang, *Chem. Commun.* **2014**,

50, 1292; c) X. Chen, M. Addicoat, S. Irle, A. Nagai, D. Jiang, *J. Am. Chem. Soc.* **2012**, *135*, 546; d) A. Nagai, Z. Q. Guo, X. Feng, S. B. Jin, X. Chen, X. S. Ding, D. L. Jiang, *Nat. Commun.* **2011**, *2*, 536.

[26] a) Z. H. Xiang, D. P. Cao, J. H. Lan, W. C. Wang, D. P. Broom, *Energ Environ. Sci.* **2010**, *3*, 1469; b) Z. H. Xiang, Z. Hu, D. P. Cao, W. T. Yang, J. M. Lu, B. Y. Han, W. C. Wang, *Angew. Chem. Int. Ed.* **2011**, *50*, 491; c) H. Furukawa, K. E. Cordova, M. O'Keeffe, O. M. Yaghi, *Science* **2013**, *341*, 974.

[27] S. Lin, C. S. Diercks, Y. B. Zhang, N. Kornienko, E. M. Nichols, Y. B. Zhao, A. R. Paris, D. Kim, P. Yang, O. M. Yaghi, C. J. Chang, *Science* **2015**, *349*, 1208.

[28] J. W. Colson, A. R. Woll, A. Mukherjee, M. P. Levendorf, E. L. Spitler, V. B. Shields, M. G. Spencer, J. Park, W. R. Dichtel, *Science* **2011**, *332*, 228.

[29] a) C. R. DeBlase, K. Hernández-Burgos, J. M. Rotter, D. J. Fortman, D. dos, S. Abreu, R. A. Timm, I. C. N. Diógenes, L. T. Kubota, H. D. Abruña, W. R. Dichtel, *Angew. Chem. Int. Ed.* **2015**, 13225; b) J. F. Van Humbeck, M. L. Aubrey, A. Alsbaiee, R. Ameloot, G. W. Coates, W. R. Dichtel, J. R. Long, *Chem. Sci.* **2015**, *6*, 5499; c) J. G. Mei, Y. Diao, A. L. Appleton, L. Fang, Z. N. Bao, *J. Am. Chem. Soc.* **2013**, *135*, 6724; d) C. Pei, T. Ben, S. Qiu, *Mater. Horiz.* **2015**, *2*, 11; e) G. S. Zhu, H. Ren, *Porous Organic Frameworks: Design, Synthesis and their Advanced Applications*, Springer, Berlin/Heidelberg, Germany **2014**; f) R. Dawson, A. I. Cooper, D. J. Adams, *Prog. Polym. Sci.* **2012**, *37*, 530; g) Y. H. Xu, S. B. Jin, H. Xu, A. Nagai, D. L. Jiang, *Chem. Soc. Rev.* **2013**, *42*, 8012.

[30] a) J. T. Zhang, Z. H. Xia, L. M. Dai, *Sci. Adv.* **2015**, *1*, e1500564; b) J. Zhang, L. Dai, *ACS Catal.* **2015**, 7244; c) L. M. Dai, Y. H. Xue, L. T. Qu, H. J. Choi, J. B. Baek, *Chem. Rev.* **2015**, *115*, 4823.

[31] K. P. Gong, F. Du, Z. H. Xia, M. Durstock, L. M. Dai, *Science* **2009**, *323*, 760.

[32] a) L. Qu, Y. Liu, J.-B. Baek, L. Dai, *ACS Nano* **2010**, *4*, 1321; b) S. Song, Y. Xue, L. Feng, H. Elbatal, P. Wang, C. N. Moorefield, G. R. Newkome, L. Dai, *Angew. Chem. Int. Ed.* **2014**, *53*, 1415.

[33] L. Zhang, J. Niu, L. Dai, Z. Xia, *Langmuir* **2012**, *28*, 7542.

[34] I. Y. Jeon, S. Zhang, L. P. Zhang, H. J. Choi, J. M. Seo, Z. H. Xia, L. M. Dai, J. B. Baek, *Adv. Mater.* **2013**, *25*, 6138.

[35] a) Q. Lin, X. Bu, A. Kong, C. Mao, F. Bu, P. Feng, *Adv. Mater.* **2015**, *27*, 3431; b) Z. S. Wu, L. Chen, J. Z. Liu, K. Parvez, H. W. Liang, J. Shu, H. Sachdev, R. Graf, X. L. Feng, K. Mullen, *Adv. Mater.* **2014**, *26*, 1450.

[36] a) J. Liu, Y. H. Xue, Y. X. Gao, D. S. Yu, M. Durstock, L. M. Dai, *Adv. Mater.* **2012**, *24*, 2228; b) J. Liu, M. Durstock, L. M. Dai, *Energy Environ. Sci.* **2014**, *7*, 1297.

[37] D. S. Yu, Y. Yang, M. Durstock, J. B. Baek, L. M. Dai, *ACS Nano* **2010**, *4*, 5633.

[38] J. Liu, G. H. Kim, Y. H. Xue, J. Y. Kim, J. B. Baek, M. Durstock, L. M. Dai, *Adv. Mater.* **2014**, *26*, 786.

[39] I. Y. Jeon, H. M. Kim, I. T. Choi, K. Lim, J. Ko, J. C. Kim, H. J. Choi, M. J. Ju, J. J. Lee, H. K. Kim, J. B. Baek, *Nano Energy* **2015**, *13*, 336.

[40] I. Y. Jeon, M. J. Ju, J. T. Xu, H. J. Choi, J. M. Seo, M. J. Kim, I. T. Choi, H. M. Kim, J. C. Kim, J. J. Lee, H. K. Liu, H. K. Kim, S. X. Dou, L. M. Dai, J. B. Baek, *Adv. Funct. Mater.* **2015**, *25*, 1170.

[41] M. J. Ju, I. Y. Jeon, K. Lim, J. C. Kim, H. J. Choi, I. T. Choi, Y. K. Eom, Y. J. Kwon, J. Ko, J. J. Lee, J. B. Baek, H. K. Kim, *Energy Environ. Sci.* **2014**, *7*, 1044.

[42] M. J. Ju, I. Y. Jeon, J. C. Kim, K. Lim, H. J. Choi, S. M. Jung, I. T. Choi, Y. K. Eom, Y. J. Kwon, J. Ko, J. J. Lee, H. K. Kim, J. B. Baek, *Adv. Mater.* **2014**, *26*, 3055.

[43] a) W. Li, Q. Li, S. Liu, C. Duan, L. Ying, F. Q. Huang, Y. Cao, *Sci China Chem.* **2015**, *58*, 257; b) L. Ye, W. Zhao zhang, H. Yao, J. Hou, *Chem. Mater.* **2014**, *26*, 3603; c) B. Liu, B. Qiu, X. Chen, L. Xiao, Y. Li, Y. He, L. Jiang, Y. Zou, *Polym. Chem.* **2014**, *5*, 5002; d) S. Li, T. Yuan, G. Tu, J. Zhang, Z. Li, *Polym. Chem.* **2015**, *54*, 7441.

[44] J. Liu, W. Zhou, J. Liu, I. Howard, G. Kilibarda, S. Schlabach, D. Coupry, M. Addicoat, S. Yoneda, Y. Tsutsui, T. Sakurai, S. Seki, Z. F. Wang, P. Lindemann, E. Redel, T. Heine, c. Woll, *Angew. Chem. Int. Ed.* **2015**, *54*, 7441.

[45] a) M. Dogru, M. Handloser, F. Auras, T. Kunz, D. Medina, A. Hartschuh, P. Knochel, T. Bein, *Angew. Chem. Int. Ed.* **2013**, *52*, 2920; b) J. Guo, Y. H. Xu, S. B. Jin, L. Chen, T. Kaji, Y. Honsho, M. A. Addicoat, J. Kim, A. Saeki, H. Ihee, S. Seki, S. Irle, M. Hiramoto, J. Gao, D. L. Jiang, *Nat. Commun.* **2013**, *4*, 2736.

[46] a) J. Li, Z. Lin, M. Alcoutlabi, X. Zhang, *Energy Environ. Sci.* **2011**, *4*, 2682; b) S.-W. Kim, D.-H. Seo, X. Ma, G. Ceder, K. Kang, *Adv. Energy Mater.* **2012**, *2*, 710; c) Z. Wang, L. Zhou, X. W. Lou, *Adv. Mater.* **2012**, *24*, 1903; d) E. Yoo, J. Kim, E. Hosono, H. Zhou, T. Kudo, I. Honma, *Nano Lett.* **2008**, *8*, 2277; e) J. Shui, F. Du, C. Xue, Q. Li, L. Dai, *ACS Nano* **2014**, *8*, 3015.

[47] a) J.-S. Park, M.-H. Lee, I.-Y. Jeon, H.-S. Park, J.-B. Baek, H.-K. Song, *ACS Nano* **2012**, *6*, 10770; b) S. Y. Bae, I. Y. Jeon, J. Yang, N. Park, H. S. Shin, S. Park, R. S. Ruoff, L. M. Dai, J. B. Baek, *ACS Nano* **2011**, *5*, 4974.

[48] J. Xu, I.-Y. Jeon, J.-M. Seo, S. Dou, L. Dai, J.-B. Baek, *Adv. Mater.* **2014**, *26*, 7317.

[49] J. Xu, J. Shui, J. Wang, M. Wang, H.-K. Liu, S. X. Dou, I.-Y. Jeon, J.-M. Seo, J.-B. Baek, L. Dai, *ACS Nano* **2014**, *8*, 10920.

[50] a) H. Liao, H. Ding, B. Li, X. Ai, C. Wang, *J. Mater. Chem. A.* **2014**, *2*, 8854; b) F. Xu, S. Jin, H. Zhong, D. Wu, X. Yang, X. Chen, H. Wei, R. Fu, D. Jiang, *Sci. Rep.* **2015**, *5*, 8225; c) X. Yang, B. Dong, H. Zhang, R. Ge, Y. Gao, H. Zhang, *RSC Adv.* **2015**, *5*, 86137; d) B. Guo, T. Ben, Z. Bi, G. M. Veith, X.-G. Sun, S. Qiu, S. Dai, *Chem. Commun.* **2013**, *49*, 4905.

[51] I. Y. Jeon, M. Choi, H. J. Choi, S. M. Jung, M. J. Kim, J. M. Seo, S. Y. Bae, S. Yoo, G. Kim, H. Y. Jeong, N. Park, J. B. Baek, *Nat. Commun.* **2015**, *6*, 7123.

[52] D. Bhattacharjya, I. Y. Jeon, H. Y. Park, T. Panja, J. B. Baek, J. S. Yu, *Langmuir* **2015**, *31*, 5676.

[53] H.-L. Jiang, B. Liu, Y.-Q. Lan, K. Kuratani, T. Akita, H. Shioyama, F. Zong, Q. Xu, *J. Am. Chem. Soc.* **2011**, *133*, 11854.